British Journal of Pharmacology

DOI:10.1111/bph.13369
www.brjpharmacol.org

RESEARCH PAPER

Functional, electrophysiological and molecular docking analysis of the modulation of $Ca_v1.2$ channels in rat vascular myocytes by murrayafoline A

S Saponara[1], M Durante[1], O Spiga[2], P Mugnai[1], G Sgaragli[1], TT Huong[3], PN Khanh[3], NT Son[3], NM Cuong[3] and F Fusi[1]

[1]Dipartimento di Scienze della Vita, Università degli Studi di Siena, Siena, Italy, [2]Dipartimento di Biotecnologie, Chimica e Farmacia, Università degli Studi di Siena, Siena, Italy, and [3]Institute of Natural Products Chemistry, Vietnam Academy of Science and Technology, Hanoi, Vietnam

Correspondence
Dr Fabio Fusi, Dipartimento di Scienze della Vita, Università degli Studi di Siena, via Aldo Moro 2, 53100 Siena, Italy.
E-mail: fabio.fusi@unisi.it

Received
7 February 2015
Revised
1 October 2015
Accepted
10 October 2015

BACKGROUND AND PURPOSE

The carbazole alkaloid murrayafoline A (MuA) enhances contractility and the Ca^{2+} currents carried by the $Ca_v1.2$ channels [$I_{Ca1.2}$] of rat cardiomyocytes. As only few drugs stimulate $I_{Ca1.2}$, this study was designed to analyse the effects of MuA on vascular $Ca_v1.2$ channels.

EXPERIMENTAL APPROACH

Vascular activity was assessed on rat aorta rings mounted in organ baths. $Ca_v1.2$ Ba^{2+} current [$I_{Ba1.2}$] was recorded in single rat aorta and tail artery myocytes by the patch-clamp technique. Docking at a 3D model of the rat, α_{1c} central pore subunit of the $Ca_v1.2$ channel was simulated *in silico*.

KEY RESULTS

In rat aorta rings MuA, at concentrations ≤14.2 μM, increased 30 mM K^+-induced tone and shifted the concentration-response curve to K^+ to the left. Conversely, at concentrations >14.2 μM, it relaxed high K^+ depolarized rings and antagonized Bay K 8644-induced contraction. In single myocytes, MuA stimulated $I_{Ba1.2}$ in a concentration-dependent, bell-shaped manner; stimulation was stable, incompletely reversible upon drug washout and accompanied by a leftward shift of the voltage-dependent activation curve. MuA docked at the α_{1C} subunit central pore differently from nifedipine and Bay K 8644, although apparently interacting with the same amino acids of the pocket. Neither Bay K 8644-induced stimulation nor nifedipine-induced block of $I_{Ba1.2}$ was modified by MuA.

CONCLUSIONS AND IMPLICATIONS

Murrayafoline A is a naturally occurring vasoactive agent able to modulate $Ca_v1.2$ channels and dock at the α_{1C} subunit central pore in a manner that differed from that of dihydropyridines.

Abbreviations

$I_{Ba1.2}$, $Ca_v1.2$ channel Ba^{2+} current; $I_{Ca1.2}$, $Ca_v1.2$ channel Ca^{2+} current; MuA, murrayafoline A; PSS, modified Krebs–Henseleit saline solution

Tables of Links

TARGETS
Ion channels
$Ca_v1.2$ channel

LIGANDS
Bay K 8644
Nifedipine

These Tables list key protein targets and ligands in this article which are hyperlinked to corresponding entries in http://www.guidetopharmacology.org, the common portal for data from the IUPHAR/BPS Guide to PHARMACOLOGY (Pawson *et al.*, 2014) and are permanently archived in the Concise Guide to PHARMACOLOGY 2013/14 (Alexander *et al.*, 2013).

Introduction

Murrayafoline A (1-methoxy-3-methyl-9H-carbazole; MuA; Figure 1) was isolated for the first time from *Murraya euchrestifolia* Hayata (Rutaceae) collected in Taiwan and identified as a carbazole alkaloid by Furukawa *et al.* (1985). Thereafter, MuA was isolated from the root of several species of the genus *Murraya* (Itoigawa *et al.*, 2000), *Glycosmis* (*Glycosmis pentaphylla* (Retz.) DC. and *Glycosmis stenocarpa* (Drake) Guilt.; Bhattacharyya and Chowdhury, 1985; Cuong *et al.*, 2004) and *Clausena* (*Clausena dunniana* Levl.; Cui *et al.*, 2002). MuA exhibits strong fungicidal activity against *Cladosporium cucumerinum* and possesses growth inhibitory activity on human fibrosarcoma HT-1080 cells as well as cell cycle M-phase inhibitory and apoptosis-inducing activity on mouse tsFT210 cells (Cui *et al.*, 2002). Furthermore, this compound provided the first example of a carbazole alkaloid able to suppress growth of the human leukemia HL-60 cell line by inducing apoptosis through the activation of the caspase-9/caspase-3 pathway (Ito *et al.*, 2012). MuA attenuated the Wnt/β-catenin pathway by promoting the degradation of intracellular β-catenin proteins (Choi *et al.*, 2010). Because molecular lesions in Wnt/β-catenin signalling and subsequent up-regulation of β-catenin response transcription occur frequently during the development of colon cancer, MuA has been proposed as a potential chemotherapeutic agent in this type of cancer.

In addition to being an interesting and promising drug *per se*, MuA represents also a useful scaffold for the design and development of novel drugs. In fact, recent results indicate that MuA derivatives containing a 1,2,3-triazole nucleus inhibit the LPS-stimulated production of pro-inflammatory cytokines (IL-6, IL-12 p40 and TNF-α) in bone marrow-derived dendritic cells, thus representing potential anti-inflammatory drugs (Thuy *et al.*, 2013). Finally, this carbazole alkaloid can be totally synthesized either from 5-methyl-2-nitrophenol, through a four-step process using the organic palladium catalysts Pd $(OAc)_2$, $Pd_2(dba)_3$ and Dave-phos (Toan *et al.*, 2013), or directly from 1,2,3,4-tetrahydrocarbazol-1-one (Chakraborty *et al.*, 2013).

MuA has been recently shown to enhance contractility and increase Ca^{2+} influx in single rat ventricular myocytes (Son *et al.*, 2014), behaving like a stimulator of $Ca_v1.2$ channels. Therefore, in view of its possible therapeutic use, it would be interesting to know its effects on vascular function. To this end, an in-depth analysis of MuA effects on rat vascular $Ca_v1.2$ channel was performed *in vitro* both on intact vessels and single myocytes and *in silico* on α_{1c} subunit pore model of the channel. MuA was shown to exert a bimodal effect on both aorta ring contractility and $I_{Ca1.2}$ and docked at the α_{1C} subunit central pore in a different way from that of the dihydropyridines.

Methods

Aorta ring preparation

All animal care and experimental protocols conformed to the European Union Guidelines for the Care and the Use of Laboratory Animals (European Union Directive 2010/63/EU) and were approved by the Italian Department of Health (666/2015-PR). All studies involving animals are reported in accordance with the ARRIVE guidelines for reporting experiments involving animals (Kilkenny *et al.*, 2010; McGrath *et al.*, 2010). A total of 74 animals were used in the experiments described here. Aorta rings (2 mm wide) were prepared from male Wistar rats (300–400 g; Charles River Italia, Calco, Italy), anaesthetized (i.p.) with a mixture of Ketavet® (30 $mg \cdot kg^{-1}$ ketamine; Intervet, Aprilia, Italy) and Xilor® (8 $mg \cdot kg^{-1}$ xylazine; Bio 98, San Lazzaro, Italy), decapitated and exsanguinated. The endothelium was removed by gently rubbing the lumen of the ring with the curved tips of a forceps. Contractile isometric tension was recorded as described elsewhere (Cuong *et al.*, 2014). Control preparations were challenged with the drug vehicle only.

Effect of MuA and Bay K 8644 on aorta rings depolarized with high K^+ concentrations

The effects of MuA and Bay K 8644 on the contraction induced by high K^+ concentrations were assessed to determine the involvement of $Ca_v1.2$ channels in their vascular activity. Steady tension was evoked in rings by either 30 mM or 60 mM K^+; thereafter, the drug under investigation was added cumulatively. At the end of each experiment, 10 μM nifedipine followed by 100 μM sodium nitroprusside were added to test muscle functional integrity. Muscle tension was evaluated as a percentage of the initial response to K^+, taken as 100%.

Effect of MuA on the concentration-response curve for K^+ of aorta rings

To study MuA-induced sensitization to K^+, a cumulative concentration-response curve to K^+ was constructed in rings

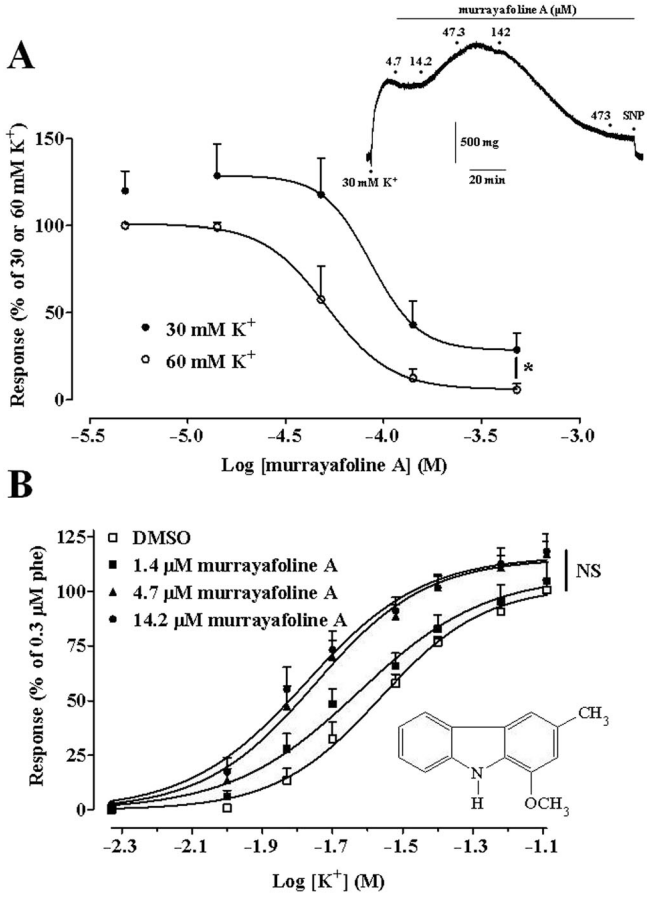

Figure 1

Effect of MuA on high K^+-induced contraction of rat aorta rings. (A) Effect of the drug on rings depolarized with either 30 mM or 60 mM K^+. Responses are shown as a percentage of the initial tension induced by 30 mM or 60 mM K^+, taken as 100%. Data points are mean ± SEM ($n = 6$). * $P < 0.05$, maximum effect at 60 mM K^+ versus that at 30 mM K^+, Student's *t* test for unpaired samples. Inset: trace (representative of six experiments) of responses to cumulative concentrations of MuA added to a ring precontracted with 30 mM K^+. The effect of 100 μM sodium nitroprusside (SNP) is also shown. (B) Concentration-response curves for K^+ in the absence (2.1 mM DMSO) or presence of various concentrations of MuA. Data points are mean ± SEM (n = 12–14) and represent the percentage of the response to 0.3 μM phenylephrine (phe), taken as 100%. The maximal responses to 80 mM K^+, recorded under the four experimental conditions, were not significantly different; one-way ANOVA and Dunnett's *post hoc* test. Inset: chemical structure of MuA.

preincubated for 15 min with vehicle or drug. Responses were evaluated as percentage of the contraction induced by 0.3 μM phenylephrine in modified Krebs–Henseleit saline solution (PSS; see below for composition), taken as 100%.

Functional interaction between MuA and Bay K 8644

Any potential interaction between MuA and Bay K 8644 at the $Ca_v1.2$ channel was assessed on depolarized rings. Rings were stimulated with 60 mM K^+ for 15 min and then washed for 90 min with a Ca^{2+}-free PSS containing 1 mM EGTA. The preparations were then challenged with 0.3 μM phenylephrine to deplete the intracellular Ca^{2+} stores. The spasmogenic response to 3 mM Ca^{2+} was assessed on rings depolarized with Ca^{2+}-free 60 mM K^+ PSS and preincubated for 30 min with the drug or vehicle. At the plateau of the Ca^{2+}-induced contraction, 10 nM Bay K 8644 followed by 100 μM sodium nitroprusside were added to test $Ca_v1.2$ channels as well as smooth muscle functional integrity. The response was evaluated as a percentage of the initial response to 60 mM K^+, taken as 100%.

Smooth muscle cell isolation procedure and whole-cell patch clamp recordings

Smooth muscle cells were freshly isolated from either the aorta, according to Zhao *et al.* (2001), or the main tail artery (Mugnai *et al.*, 2014). Briefly, a 3 mm long thoracic section of aorta was incubated at 37°C in 2 mL of Ca^{2+}-free external solution (see below) containing 20 mM taurine (prepared by replacing NaCl with equimolar taurine), 1 mg·mL^{-1} bovine serum albumin, 0.75 mg·mL^{-1} papain and 1 mg·mL^{-1} DL-dithiothreitol, and gently bubbled with a 95% O_2–5% CO_2 gas mixture for 20–30 min. After removing the adventitia, the aorta was cut into small pieces and transferred into a Ca^{2+}-free external solution containing 20 mM taurine, 1 mg·mL^{-1} collagenase (type XI) and 1 mg·mL^{-1} hyaluronidase for 10 min at 37°C. Single cells were released by gentle trituration of minced, proteolysed tissue, through a Pasteur pipette, stored at 4°C in the Ca^{2+}-free external solution containing 20 mM taurine and used on the same day of the preparation.

Smooth muscle cells were freshly isolated from a 5 mm long piece of main tail artery incubated at 37°C in 2 mL of 20 mM taurine and 0.1 mM Ca^{2+} external solution containing 1 mg·mL^{-1} collagenase (type XI), 1 mg·mL^{-1} soybean trypsin inhibitor and 1 mg·mL^{-1} BSA, gently bubbled with a 95% O_2–5% CO_2 gas mixture, as previously described (Fusi *et al.*, 2001). Cells, stored in 0.05 mM Ca^{2+} external solution containing 20 mM taurine and 0.5 mg·mL^{-1} BSA at 4°C under normal atmosphere, were used for experiments within 2 days after isolation (Mugnai *et al.*, 2014).

Whole-cell patch-clamp recordings

Cells were continuously superfused with external solution containing 0.1 mM Ca^{2+} and 30 mM tetraethylammonium using a peristaltic pump (LKB 2132, Bromma, Sweden), at a flow rate of 400 μL·min^{-1}. The conventional whole-cell patch-clamp method (Hamill *et al.*, 1981) was employed to voltage-clamp smooth muscle cells, as previously described (Cuong *et al.*, 2014; see also Supporting Information). Electrophysiological responses were assessed at room temperature (20–22°C).

$I_{Ba1.2}$ and $I_{Ca1.2}$ recordings

The current carried by the $Ca_v1.2$ channels, $I_{Ba1.2}$ or $I_{Ca1.2}$, was always recorded in external solution containing 30 mM tetraethylammonium and 5 mM Ca^{2+} or Ba^{2+} (tail artery) or 10 mM Ba^{2+} (aorta). Current was elicited with 250 ms clamp pulses (0.067 Hz) to 0 mV from a V_h of −50 mV (tail artery) or to 10 mV from a V_h of −80 mV (aorta). Data were collected once the current amplitude had been stabilized (usually 7–10 min after the whole-cell configuration had been obtained) by

using pClamp 8.2.0.232 (Molecular Devices Corporation, Sunnyvale, CA, USA). At this point, the various protocols were performed as detailed below. $I_{Ba1.2}$ and $I_{Ca1.2}$ did not run down during the following 40 min under these conditions (Fusi *et al.*, 2012).

Steady-state inactivation and activation curves were obtained as previously described (Mugnai *et al.*, 2014; see also Supporting Information).

K^+ currents were blocked with 30 mM tetraethylammonium in the external solution and Cs^+ in the internal solution. Current values were corrected for leakage using 10 μM nifedipine, which completely blocked $I_{Ba1.2}$ and $I_{Ca1.2}$.

Data analysis

Data are reported as mean ± SEM; *n* is the number of cells or rings analysed (indicated in parentheses), isolated from at least three animals. Analysis of data was accomplished by using pClamp 9.2.1.8 software (Molecular Devices Corporation) and GraphPad Prism version 5.04 (GraphPad Software Inc., San Diego, CA, USA). The AUC, used as a cumulative measurement of drug effect, was calculated to compare the concentration-response curves recorded at 30 mM and 60 mM K^+. The area was computed, using the trapezoid rule, in units of the X axis multiplied by the units of the Y axis.

Statistical analyses and significance as measured by one-way or repeated measures ANOVA (followed by either Dunnett's or Bonferroni's *post hoc* test), one sample *t* test or Student's *t* test for paired or unpaired samples (two-tailed) were obtained using GraphPad InStat version 3.06 (GraphPad Software, USA). *Post hoc* tests were performed only when ANOVA found a significant value of F and no variance in homogeneity. In all comparisons, $P < 0.05$ was considered significant. The pharmacological response to each substance was described in terms of either pEC_{50} or pIC_{50}.

Solutions and materials

The PSS contained (in mM): NaCl 118; KCl 4.75; KH_2PO_4 1.19; $MgSO_4$ 1.19; $NaHCO_3$ 25; glucose 11.5; $CaCl_2$ 2.5; gassed with a 95% O_2–5% CO_2 gas mixture to a pH of 7.4. PSS containing KCl at a concentration greater than 4.75 mM was prepared by replacing NaCl with equimolar KCl.

External solution contained (in mM): 130 NaCl, 5.6 KCl, 10 HEPES, 20 glucose, 1.2 $MgCl_2$ and 5 Na-pyruvate; pH 7.4. The internal solution contained (in mM) 100 CsCl, 10 HEPES, 11 EGTA, 1 $CaCl_2$ (pCa 8.4), 2 $MgCl_2$, 5 Na-pyruvate, 5 succinic acid, 5 oxalacetic acid, 3 Na_2-ATP and 5 phosphocreatine; pH was adjusted to 7.4 with CsOH.

The osmolarity of the tetraethylammonium- and Ca^{2+} or Ba^{2+}-containing external solution (320 mosmol) and that of the internal solution (290 mosmol; Stansfeld and Mathie, 1993) was measured with an osmometer (Osmostat OM 6020, Menarini Diagnostics, Florence, Italy).

Phenylephrine, ACh, collagenase (type XI), trypsin inhibitor, bovine serum albumin, papain, DL-dithiothreitol, hyaluronidase, tetraethylammonium chloride, EGTA, HEPES, taurine, Bay K 8644 (methyl (4S)-2,6-dimethyl-5-nitro-4-[2-(trifluoromethyl)phenyl]-1,4-dihydropyridine-3-carboxylate) and nifedipine were from Sigma Chimica (Milan, Italy); sodium nitroprusside was from Riedel-De Haën AG (Seelze-Hannover, Germany). MuA was isolated from the dried, powdered roots of *Glycosmis stenocarpa* (Drake) Guilt., as previously described (Cuong *et al.*, 2004). MuA (473 mM stock solution), dissolved directly in DMSO, Bay K 8644 and nifedipine, dissolved in ethanol, were diluted at least 1000 times prior to use. All these solutions were stored at −20°C and protected from light by wrapping containers with aluminium foil. The resulting concentrations of DMSO and ethanol (below 0.1%, v v^{-1}) did not affect responses of the preparations. Phenylephrine was dissolved in 0.1 M HCl. Sodium nitroprusside was dissolved in distilled water. All other substances used were of analytical grade and used without further purification.

Docking experiments

Construction of the model. The rat $Ca_v1.2$ channel α_{1C} subunit sequence (NP_036649.2) was retrieved from the NCBI Protein Database (http://www.ncbi.nlm.nih.gov/protein/). This has four repeats, each containing six transmembrane helices (S1–S6) and a P-loop between S5 and S6 (Cheng *et al.*, 2009). The quality of a homology model is given by the accuracy of the sequence alignment and the resolution of the template structures used. A PSI-BLAST search (Altschul *et al.*, 1997) for rat α_{1C} subunit sequences was firstly performed in order to obtain the best template of the unit and the tetrameric portion of the model. Subsequently, the sequences were aligned as previously reported (Zhorov and Tikhonov, 2004; Cheng *et al.*, 2010). Here, the disposition of both P-loops and inner helices was derived from earlier structure templates. Therefore, complete, suitable templates were the K_vAP (1ORQ pdb) (Jiang *et al.*, 2003) and the K_vAP (2R9R pdb) for the reconstruction of the unit and the tetramer respectively.

When viewed from the extracellular side, the repeats I–IV were arranged clockwise around the central pore (Cheng *et al.*, 2009). This channel model was built using the SwissPdbViewer-DeepView version 4.1 (Guex and Peitsch, 1997), which allowed us also to define the consistency of bond distances, bond angles and torsion angles with the values of standard proteins. The structure of the channel model was energetically minimized using the Gromacs package (Berendsen *et al.*, 2012) equipped with the AMBER force field (Sorin and Pande, 2005) till a final convergence of 0.01 kcal mol^{-1} $Å^{-1}$ was achieved. The stereochemical quality of the final structure (i.e. the distribution of ϕ and ψ angles) was assessed by means of PROCHECK program (Laskowski *et al.*, 1993). With this test, no severely disallowed atomic contacts were detected, suggesting essentially good stereochemistry, with 86.1% and 11.0% of the amino acid residues in the most favoured and additional allowed regions, respectively, and with 2.1% and 0.8% residues in generously allowed and disallowed regions of the Ramachandran plot.

Docking simulations. Docking of ligands (nifedipine, Bay K 8644 and MuA) was simulated by using flexible side chains protocol with AutoDock/Vina version 1.1 (Trott and Olson, 2010). This program used an iterated local search global optimizer algorithm based on a succession of steps, which consisted of mutation and local optimization. Ligand structures were retrieved from the PubChem database (http://www.ncbi.nlm.nih.gov/pcsubstance/), and pdbqt files were generated by using scripts included in the

Molecular Graphics Laboratory (MGL) tools (Morris *et al.*, 2009). The generation and affinity grid maps, view of docking poses and analysis of virtual screening results were carried out by using AutoDock plug-in of PyMOL. The dimensions of the box for docking calculation (60 Å × 60 Å × 60 Å) were sufficiently great to include not only the active docking site, as previously suggested (Cosconati *et al.*, 2007), but also significant portions of the surrounding surface.

In silico alanine scanning mutagenesis was performed by using the ABS-Scan tool 2 (Anand *et al.*, 2014). Each amino acid residue present at the binding site was computationally mutated to alanine and the ligand interaction energy recalculated for each mutant. The corresponding ΔΔG values were computed by comparing them with the wild type protein, thus allowing the evaluation of individual residue contribution towards ligand interaction.

Results

Effect of MuA on aorta rings contracted by high K^+ concentrations

To determine the involvement of $Ca_v1.2$ channels in the vascular activity of MuA, its effect was evaluated on the contraction induced by both 30 mM and 60 mM K^+ in aorta rings. As shown in Figure 1A, MuA caused a concentration-dependent relaxation of the preparations. Rings contracted by 60 mM K^+ relaxed fully in the presence of 473 μM MuA with a pIC_{50} value of 4.22 ± 0.13 (n = 6) and an AUC value of 109.6 ± 13.0. Furthermore, maximal relaxation was significantly greater than that recorded in preparations contracted by phenylephrine (see Supporting Information Fig. S1; $P < 0.05$, Student's t test for unpaired samples). When rings were depolarized with 30 mM K^+, the concentration-response curve was shifted upward (Figure 1A), showing an AUC value of 180.5 ± 25.3 (n = 6; $P < 0.05$ Student's t test for unpaired samples). MuA, at concentrations ≤47.3 μM, caused an increase in K^+-induced vascular tone while at higher concentrations, partly reversed the contraction, showing a relative pIC_{50} value of 4.07 ± 0.10 μM (n = 6).

Murrayafoline A potentiated, in a concentration-dependent manner, the contractile response to K^+ (Figure 1B) causing a leftward shift of the K^+ concentration-response curve. pEC_{50} values for K^+ changed from 1.61 ± 0.04 (2.1 mM DMSO; n = 12) to 1.67 ± 0.04 (1.4 μM MuA, n = 13; $P > 0.05$, Dunnett's *post hoc* test), 1.78 ± 0.04 (4.7 μM MuA, n = 14; $P < 0.05$) and 1.80 ± 0.05 (14.2 μM MuA, n = 14; $P < 0.05$). Potentiation of responses to K^+ by 14.2 μM MuA was greater at 15 mM K^+, being 409.6% of control, as compared with that observed at higher K^+ concentrations (157.0% and 124.3% at 30 mM and 60 mM K^+ respectively). MuA, however, did not modify the maximal response to K^+.

Effect of Bay K 8644 on aorta rings contracted by high K^+ concentrations and its interaction with MuA

To define the effects of MuA on aorta rings, the same experiments described earlier were repeated, using the $Ca_v1.2$ channel agonist Bay K 8644 instead of MuA. When the effect of Bay K 8644 on the contraction induced by high K^+ concentrations was evaluated in aorta rings, a concentration-dependent and marked increase of muscle tone in preparations contracted by 30 mM K^+ was observed, whilst in rings contracted by 60 mM K^+, this was considerably smaller (Figure 2A). The AUC values were 214.3 ± 36.7 (n = 7) and 91.1 ± 20.6 (n = 6; $P < 0.05$ Student's t test for unpaired samples) respectively.

Any potential pharmacological interactions between MuA and Bay K 8644 were assessed in rings contracted by the addition of 3 mM Ca^{2+} to the Ca^{2+}-free, 60 mM K^+-containing PSS. In rings pre-treated with DMSO, 10 nM Bay K 8644 increased Ca^{2+}-induced contraction by about 40% (Figure 2B). MuA, at concentrations of 47.3 μM and

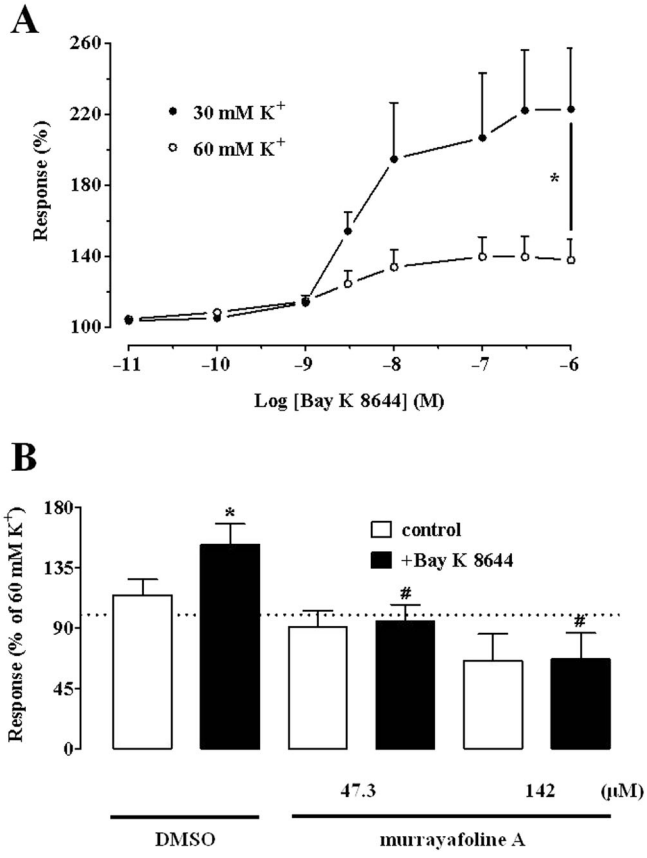

Figure 2

Effect of Bay K 8644 on high K^+-induced contraction of rat aorta rings and its functional interaction with MuA. (A) Concentration-response curves of Bay K 8644 in rings depolarized with 30 mM or 60 mM K^+. Responses are shown as percentage of the initial tension induced by 30 mM or 60 mM K^+, taken as 100%. Data points are mean ± SEM (n = 6–7). * $P < 0.05$ maximum effect at 30 mM K^+ versus that at 60 mM K^+; Student's t test for unpaired samples. (B) Effect of 10 nM Bay K 8644 on Ca^{2+}-induced vascular tone of depolarized rings treated with either vehicle (DMSO) or MuA. Columns are mean ± SEM (n = 7–10) and represent the percentage of the response to 60 mM K^+, taken as 100%. * $P < 0.05$ versus control; Student's t test for paired samples; # $P < 0.05$ versus DMSO + Bay K 8644; one-way ANOVA and Dunnett's *post hoc* test.

142 μM, significantly antagonized the Bay K 8644-induced increase.

Ca^{2+} influx stimulated by $Ca_v1.2$ channel agonists may be completely buffered by the superficial sarcoplasmic reticulum or even prevented if channels are not pre-activated with low K^+ concentrations. However, addition of MuA to rings either bathed in normal PSS or pre-treated with 1 μM thapsigargin or 15 mM K^+ failed to induce mechanical responses (data not shown). When this assay was performed with Bay K 8644, in normal PSS, a concentration-dependent contraction was recorded in seven out of 17 preparations (pEC_{50} value of 7.53 ± 0.24, n = 7). In rings pre-incubated with 15 mM K^+ or 1 μM thapsigargin, the concentration-response curves to Bay K 8644 shifted to the left (pEC_{50} value of 8.33 ± 0.19, n = 11, $P > 0.05$ and 9.13 ± 0.41, n = 6, $P < 0.05$, Dunnett's *post hoc* test). In the former case (15 mM K^+), an increase in drug efficacy was also observed (data not shown).

Effect of MuA on $I_{Ba1.2}$ and $I_{Ca1.2}$

The contribution of $Ca_v1.2$ channel modulation to the effects of MuA on vascular rings was assessed on $I_{Ba1.2}$ recorded in isolated aorta myocytes. At V_h of −80 mV, MuA stimulated the current in a concentration-dependent manner with a pEC_{50} value of 5.33 ± 0.08 (n = 7) (Figure 3A). At 47.3 μM this stimulatory effect was less evident, whilst at 473.4 μM, MuA clearly inhibited $I_{Ba1.2}$. Similar results (pEC_{50} value of 5.26 ± 0.10, n = 7; $P > 0.05$) were obtained in tail artery myocytes. Therefore, an in-depth analysis of MuA effects on $I_{Ba1.2}$ was performed on the latter cells, whose biophysical and pharmacological properties are well characterized (Mugnai *et al.*, 2014 and references therein). MuA modulation of the current through $Ca_v1.2$ channels was not affected by changes of either the charge carrier or V_h. In fact, when equimolar Ca^{2+} replaced Ba^{2+} in the external solution or when V_h was changed to −50 mV, the stimulatory potency was not modified (pEC_{50} 5.60 ± 0.12, n = 5 and 5.44 ± 0.03, n = 9, respectively; $P > 0.05$).

$I_{Ba1.2}$ evoked at 0 mV from a V_h of −50 mV activated and then declined with time courses that could be fitted by a mono-exponential function. MuA did not affect significantly either the τ for inactivation or that for activation at all concentrations tested (data not shown).

Figure 3B shows the time course of the effects of MuA on $I_{Ba1.2}$ recorded from V_h of −50 mV to a test potential of 0 mV. After the current had reached steady values, the addition to bath solution of 14.2 μM MuA produced a gradual increase of the current that reached a plateau in about 4 min. Current amplitude stimulation was only partially reversible upon drug washout but still blocked by the Ca^{2+} antagonist nifedipine. Furthermore, MuA-induced stimulation of $I_{Ba1.2}$ was stable for about 30 min.

The current–voltage relationships recorded at V_h of −50 mV (Figure 4A) show that 14.2 μM MuA significantly increased the peak $I_{Ba1.2}$ without altering either the maximum at 10 mV or the threshold at approximately −30 mV. The relative value of $I_{Ba1.2}$ stimulation by MuA (Figure 4, inset) was constant in the range of membrane potential values of −20 to 30 mV. In addition, drug washout partially reversed MuA-induced stimulation of $I_{Ba1.2}$ at most of the tested membrane potentials.

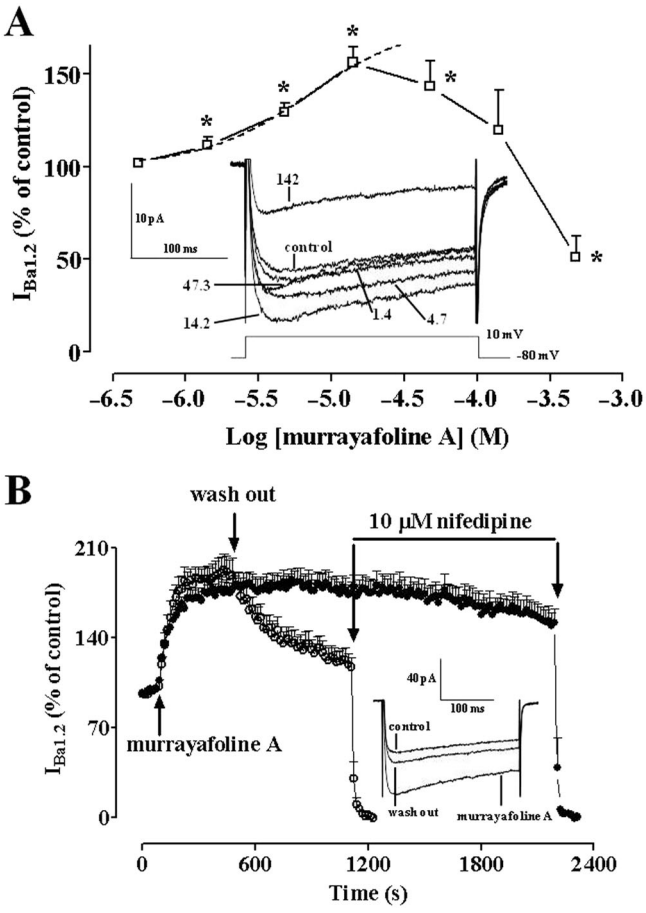

Figure 3

Modulation by murrayafoline A of $I_{Ba1.2}$ of single rat aorta myocytes. (A) Concentration-dependent effect of MuA at the peak of $I_{Ba1.2}$ trace in aorta myocytes. The curve shows the best fit of the points. Responses are shown as percentage of control. Data points are mean ± SEM (n = 7). * $P < 0.05$ versus control; one sample t test. Inset: average traces (recorded from seven cells) of conventional whole-cell $I_{Ba1.2}$ elicited with 250 ms clamp pulses to 10 mV from a V_h of −80 mV (see schematic diagram), measured in the absence (control) or presence of various concentrations (μM) of MuA. (B) Time course of $I_{Ba1.2}$ stimulation induced by MuA and drug washout. MuA (14.2 μM) was applied at the time indicated by the arrow, and current was recorded during a typical depolarization from −50 to 0 mV, applied every 15 s (0.067 Hz) and subsequently normalized to the current recorded just prior to MuA addition. Drug washout allowed for partial recovery from stimulation. $I_{Ba1.2}$ suppression by 10 μM nifedipine is also shown. Data points are mean ± SEM (n = 7–9). Inset: average traces (recorded from seven cells) of conventional whole-cell $I_{Ba1.2}$ elicited with 250 ms clamp pulses to 0 mV from a V_h of −50 mV, recorded in the absence (control) or presence of 14.2 μM MuA as well as after drug washout.

Effects of MuA on steady-state inactivation and activation curves for $I_{Ba1.2}$

The voltage dependence of MuA-induced current modulation was further investigated by analysing the steady-state inactivation and activation curves for $I_{Ba1.2}$. MuA (14.2 μM) failed to affect both the 50% inactivation potential (−17.88 ± 1.27 mV, control and −19.96 ± 1.66 mV, MuA; n = 6; $P > 0.05$,

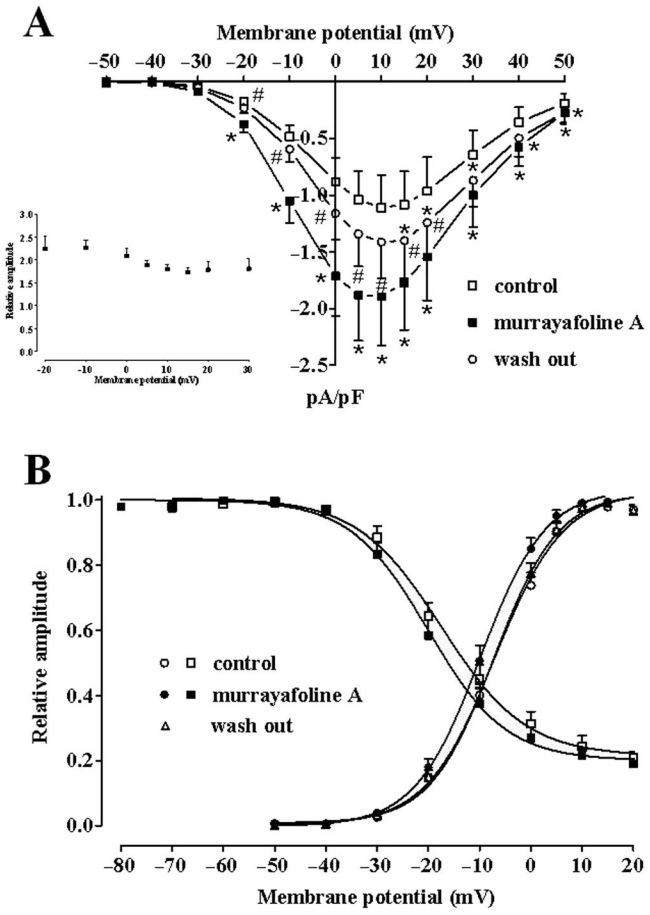

Figure 4

Effect of MuA on $I_{Ba1.2}$–voltage relationship as well as on $I_{Ba1.2}$ activation and inactivation curves. (A) Effect of MuA on the current–voltage relationship. Current–voltage relationships, recorded from a V_h of −50 mV, constructed prior to the addition of drug (control), in presence of 14.2 μM MuA and after drug wash out. Data points are mean ± SEM (n = 7). * $P < 0.05$ versus control. # $P < 0.05$ versus MuA; repeated measures ANOVA and Bonferroni's *post hoc* test. Inset: relationship between membrane potential and relative value of $I_{Ba1.2}$ stimulation by 14.2 μM MuA. Current stimulation was expressed as a fold increase over the peak amplitude of $I_{Ba1.2}$ evoked, in the absence of MuA, by varying the amplitude of depolarizing pulse. Data points are mean ± SEM (n = 7). $P > 0.05$; one-way ANOVA and Bonferroni's *post hoc* test. (B) Steady-state inactivation curves recorded from V_h of −50 mV, obtained in the absence (control) and presence of 14.2 μM MuA, were fitted to the Boltzmann equation. The current measured during the test pulse was plotted against membrane potential and expressed as relative amplitude. Activation curves obtained from the current–voltage relationships of panel A and fitted to the Boltzmann equation. Data points are mean ± SEM (n = 6–7).

Student's t test for paired samples) and the slope factor (−7.57 ± 0.16 mV and −7.62 ± 0.64 mV; $P > 0.05$) of the steady-state inactivation curve (Figure 4B).

The activation curves, calculated from the current–voltage relationships showed in Figure 4A, were fitted to the Boltzmann equation. MuA significantly decreased the 50% activation potential (−6.65 ± 1.24 mV, control and −9.47 ± 1.18 mV, MuA, n = 6; $P < 0.05$, repeated measures ANOVA and Dunnett's *post hoc* test) without changing the slope factor (6.65 ± 0.51 mVand 6.32 ± 0.32 mV; Figure 4B). Drug washout fully reversed this effect (50% activation potential −7.07 ± 1.08 mVand slope factor 6.14 ± 0.28 mV; $P > 0.05$).

Modelling and docking

To determine *in silico* the interaction of MuA with the $Ca_v1.2$ channel protein, the homology model of the central pore of the rat α_{1c} subunit was reconstructed in accordance with Cheng *et al.* (2009). Docking calculations performed with the reference dihydropyridines, nifedipine and Bay K 8644, showed similar ΔG values (Table 1). Moreover, the two molecules positioned inside the pocket in a superimposable manner (Figure 5A). By interacting with specific parts of the channel pore, nifedipine and Bay K 8644 formed H-bonds with the same key dihydropyridine-sensing amino acid residues of three different helices (Figure 5B): Tyr^{1178} (IIIS6) with the NH group and Gln^{1069} (IIIS5) and Tyr^{1489} (IVS5) with the $COOCH_3$ groups. On the contrary, MuA, which showed a less favourable ΔG value (Table 1), had a different pose (Figure 5A) characterized by the absence of H-bonds (Figure 5B).

In silico alanine scanning mutagenesis gave rise to remarkably similar ΔΔG values for both nifedipine and Bay K 8644 (Figure 5C), whereas MuA exhibited a rather different profile, some residues even appearing unfavourable to its binding.

Functional interaction between MuA and Bay K 8644 or nifedipine on $I_{Ba1.2}$

Because docking analysis suggested that MuA binds the $Ca_v1.2$ channel binding pocket at a site that can bind also nifedipine and Bay K 8644, the functional interaction between this alkaloid and the two dihydropyridines was investigated. Bay K 8644 (100 nM) stimulated $I_{Ba1.2}$ in the range from −30 to 50 mV and shifted the maximum of the current–voltage relationships by 10 mV in the hyperpolarizing direction (Figure 6A). The activation curves, calculated from the current–voltage relationships shown in Figure 6A, were fitted to the Boltzmann equation. Bay K 8644 significantly decreased the 50% activation potential (−5.72 ± 0.72 mV, control and −13.95 ± 0.82 mV, Bay K 8644, n = 6; $P < 0.05$, repeated measures ANOVA and Dunnett's *post hoc* test) and changed the slope factor (from 6.22 ± 0.30 mV to 4.67 ± 0.26 mV; $P < 0.05$) (Figure 6A inset). The subsequent addition of 14.2 μM MuA did not modify Bay K 8644-induced effects on both $I_{Ba1.2}$ amplitude and activation curve (50% activation potential −13.71 ± 0.57 mV and slope factor 5.20 ± 0.20 mV; $P > 0.05$).

Under control conditions, the current evoked at 0 mV from a V_h of −50 mVactivated and then declined with time courses that could be fitted by mono-exponential functions (Figure 6B). Bay K 8644 (100 nM) significantly prolonged the τ for activation and reduced that for inactivation: the subsequent addition of MuA brought only the τ for activation almost to control values, without affecting that for inactivation.

The antagonistic effect of nifedipine was determined under control conditions as well as in myocytes pre-treated with MuA or Bay K 8644. Nifedipine inhibited $I_{Ba1.2}$ in a concentration-dependent manner with a pIC_{50} value of 7.67 ± 0.06 (n = 6; Figure 7A,D). Similar results were obtained in the presence of 14.2 μM MuA (pIC_{50} value of 7.60 ± 0.10, n = 6; $P > 0.05$, one-way ANOVA and Dunnett's *post hoc* test;

Table 1

Murrayafoline A, nifedipine and Bay K 8644 docking at the channel pore of rat $Ca_v1.2$ α_{1C} subunit

Molecule	ΔG_{bind}	Surrounding amino acid residues
Murrayafoline A ($C_{14}H_{13}NO$)	−6.9	Ser1141 (IIIP), **Gln1069 (IIIS5)**, **Tyr1489 (IVS6)**, **Ile1486 (IVS6)**, Met1490 (IVS6), **Met1186 (IIIS6)**, **Phe1138 (IIIP)**, Ile1182 (IIIS6), **Thr1066 (IIIS5)**, **Leu1137 (IIIP)**, Thr1142 (IIIP), Tyr1178 (IIIS6), **Met1134 (IIIP)**, Ile1189 (IIIS6), **Phe1070 (IIIS5)**, Phe1485 (IVS6)
Nifedipine ($C_{17}H_{18}N_2O_6$)	−7.9	
Bay K 8644 ($C_{16}H_{15}F_3N_2O_4$)	−8.0	

ΔG_{bind} is the free-energy of binding estimated from the top of 20 cluster results and given in kcal mol^{-1}. Surrounding residues refer to amino acid residues of the four repeats (in parentheses) in the binding pocket region interacting with and located within 5 Å from any atom of the docked ligands. In bold are represented the amino acid residues of the binding pocket segments engaged by the three ligands and specifically involved in the binding interaction according to the best poses of the different, calculated cluster solutions.

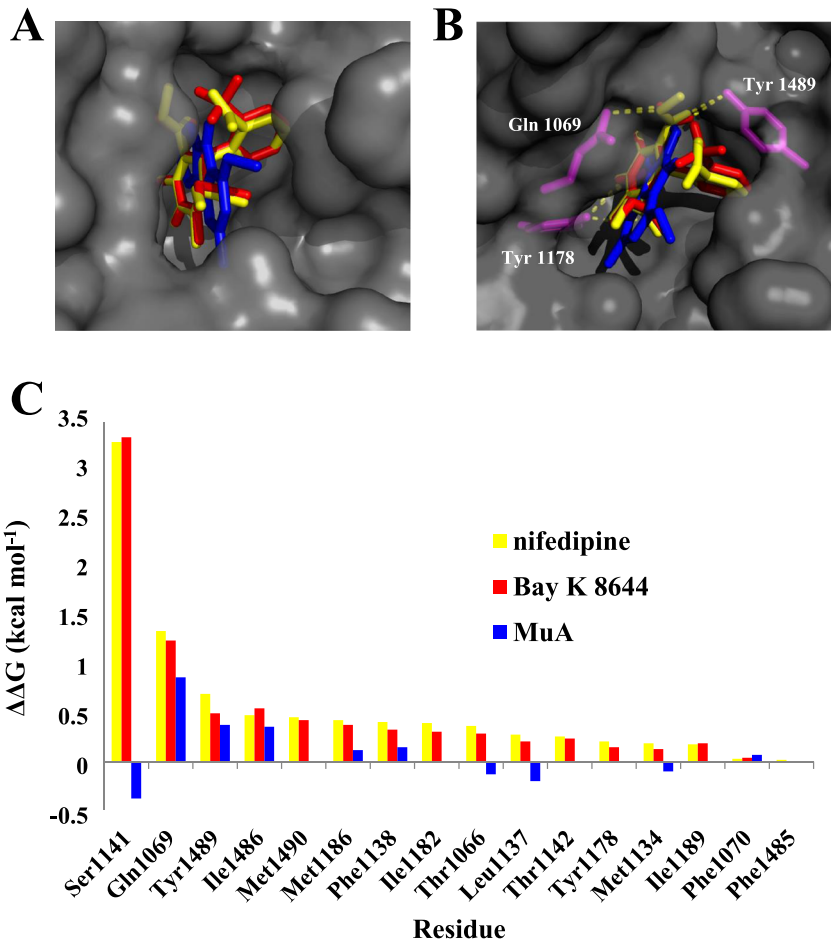

Figure 5

Docking of murrayafoline A, nifedipine and Bay K 8644 at the $Ca_v1.2$ channel α_{1C} subunit model and effect of alanine scanning mutagenesis. (A) Docked structures of nifedipine (yellow), MuA (blue) and Bay K 8644 (red), displayed as bold sticks, in the pore channel, displayed as molecular surface coloured grey. (B) Best docking poses of the three ligands; the pore amino acid residues [Gln1069 (IIIS5), Tyr1178 (IIIS6) and Tyr1489 (IVS5)] forming H-bonds with nifedipine and Bay K 8644 are displayed in magenta. (C) ABS-scan energy ploy. ΔΔG values recorded after alanine mutation of the single residues involved in the binding of nifedipine, Bay K 8644 and MuA. Amino acid residues are listed in rank order according to their contribution in the complex with nifedipine and Bay K 8644 (ΔΔG values).

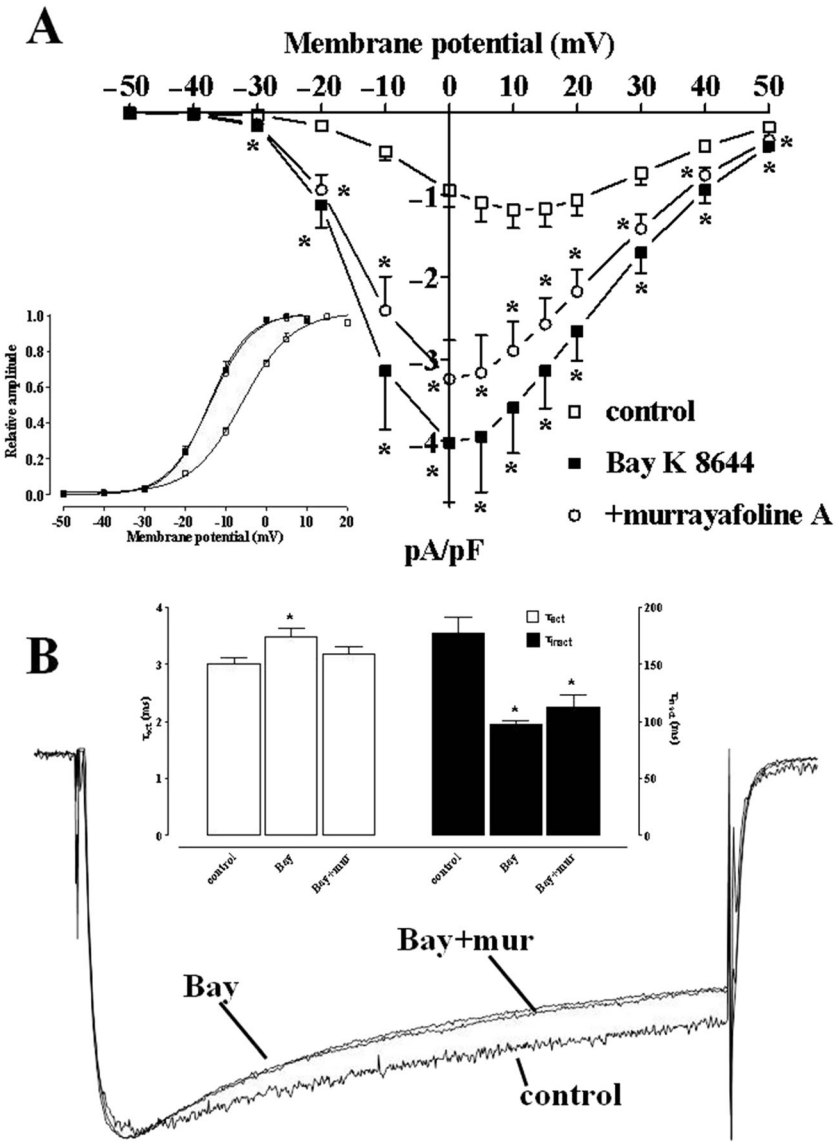

Figure 6

Effects of Bay K 8644 and murrayafoline A on $I_{Ba1.2}$–voltage relationship and kinetics in rat tail artery myocytes. (A) Current–voltage relationships constructed prior to the addition of drugs (control), in the presence of 100 nM Bay K 8644 and in the presence of Bay K 8644 plus 14.2 μM MuA. Data points are mean ± SEM (n = 6). * $P < 0.05$ versus control, $P > 0.05$ Bay K 8644 versus +murrayafoline A, repeated measures ANOVA and Bonferroni's *post hoc* test. Inset: steady-state activation curves obtained from the current–voltage relationships of panel A and fitted to the Boltzmann equation (see Methods section). (B) Average traces (recorded from six cells) of conventional whole-cell $I_{Ba1.2}$ elicited with 250 ms clamp pulses to 0 mV from a V_h of −50 mV, recorded in the absence (control) or presence of 100 nM Bay K 8644 (Bay) and Bay K 8644 plus 14.2 μM MuA (Bay + mur). Control and Bay K 8644 plus MuA traces are magnified so that the peak amplitude matched that of Bay K 8644. Inset: time constant for activation (τ_{act}) and for inactivation (τ_{inact}) measured in the absence (control) or presence of Bay K 8644 (Bay) and Bay K 8644 plus MuA. Columns represent mean ± SEM (n = 6). * $P < 0.05$ versus control, repeated measures ANOVA and Bonferroni's *post hoc* test.

Figure 7B,D). On the contrary, when $I_{Ba1.2}$ was stimulated with 100 nM Bay K 8644, the concentration-response curve to nifedipine was shifted to the right (pIC_{50} value of 6.42 ± 0.08, n = 7; $P < 0.05$; Figure 7C,D).

Discussion

Murrayafoline A has been shown recently to enhance contractility and increase Ca^{2+} influx in single rat ventricular myocytes (Son *et al.*, 2014), behaving like a stimulator of $Ca_v1.2$ channels. However, its effects on vascular function are unknown. The present investigation demonstrated that MuA was able either to stimulate or to inhibit contraction of vascular smooth muscle by directly activating or blocking $Ca_v1.2$ channels, respectively, depending on the concentration used. This conclusion is supported not only by indirect, functional observations but also by direct electrophysiological data and docking analysis.

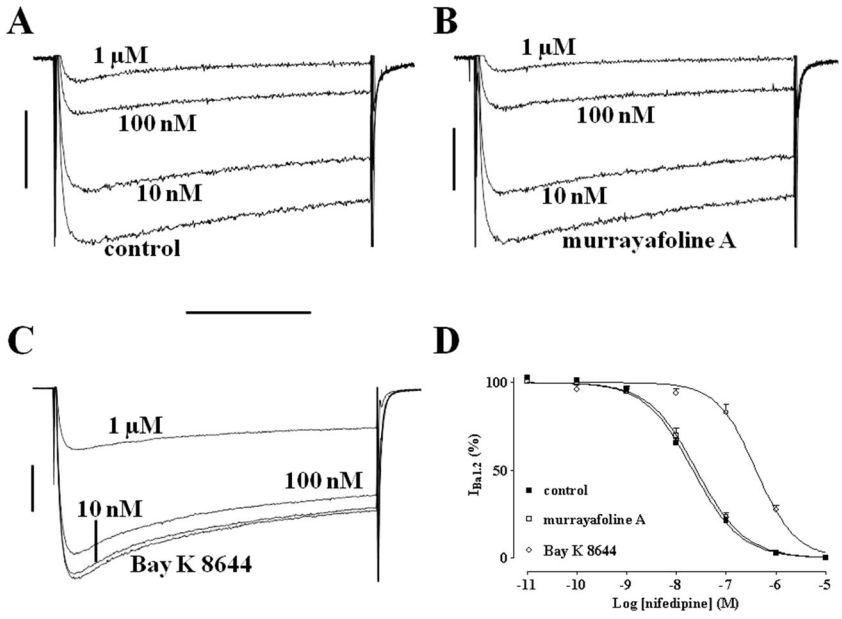

Figure 7

Effects of nifedipine on Bay K 8644- or murrayafoline A-induced stimulation of $I_{Ba1.2}$ in rat tail artery myocytes. (A–C) Average traces (recorded from six to seven cells) of conventional whole-cell $I_{Ba1.2}$ elicited with 250 ms clamp pulses to 0 mV from a V_h of −50 mV and recorded after the addition of cumulative concentrations (10 nM-1 μM) of nifedipine (A) in the absence (control) or presence of (B) 14.2 μM MuA and (C) 100 nM Bay K 8644. (D) Amplitude of the current normalized upon that recorded under control conditions and in the presence of either MuA or Bay K 8644, taken as 100%. The curves show the best fit of the points. Data points are mean ± SEM (n = 6–7).

The mechanical and electrophysiological effects of MuA were compared with those of the synthetic $Ca_v1.2$ channel activator Bay K 8644 (Hess *et al.*, 1984). Both vascular smooth muscle active tone and $I_{Ba1.2}$ stimulation induced by MuA shared some basic features with those sustained by Bay K 8644. Thus, MuA, like Bay K 8644, stimulated the active tone of aorta rings depolarized with 30 mM K^+, this effect disappearing when K^+ concentration raised up to 60 mM (i.e. in fully activated preparations). Furthermore, it shifted the K^+ concentration-response curve to the left without changing its maximum (for Bay K 8644, see Fusi *et al.*, 2003). Finally, at low concentrations, both drugs stimulated $I_{Ba1.2}$ in a nifedipine-sensitive manner. Collectively, these findings suggest that MuA, like Bay K 8644, affected the vascular $Ca_v1.2$ channel protein.

Murrayafoline A, added either before or after K^+, enhanced tissue responses to low, but not to high depolarizing stimuli. 'Sensitization' to K^+ is generally observed with drugs, like Bay K 8644, that facilitate the voltage-dependent activation of $Ca_v1.2$ channels (this paper), thus shifting the curve relating tension development and depolarizing stimulus (i.e. membrane potential) to lower K^+ concentrations (i.e. more negative values; see Fusi *et al.*, 2003). This hypothesis was confirmed by the Boltzmann analysis (activation curve) of the current–voltage relationship, showing that MuA, similarly to Bay K 8644, significantly decreased the 50% activation potential of $I_{Ba1.2}$.

Murrayafoline A caused a parallel leftward shift of the K^+ concentration-response curve as well as a relatively constant stimulation of current amplitude over a broad range of membrane potentials. These data suggested that the drug most likely increased the open probability of the channel and that its action on the channel was voltage-independent. However, only single-channel recordings comparing the effect of Bay K 8644 and MuA may provide direct evidence for this possibility.

Ca^{2+} channel activators, such as Bay K 8644, are able to evoke full contractile, tonic responses in vascular smooth muscle preparations, mainly when they are depolarized with low K^+ concentrations (this paper; Usowicz *et al.*, 1995; Fusi *et al.*, 2003) or when the Ca^{2+} buffering activity of the superficial sarcoplasmic reticulum is impaired (this paper; Asano and Nomura, 1999). This means that, on one hand, $Ca_v1.2$ channel activation is voltage-dependent, and therefore, channels have to be activated in order to respond to Ca^{2+}-agonist drugs. On the other hand, Ca^{2+} influx triggered by the Ca^{2+}-agonist drug can induce a maximum muscle contraction only in the absence of a functional sarcoplasmic reticulum. MuA, however, did not elicit significant mechanical responses in rat aorta rings either under control conditions or in the presence of thapsigargin or moderate concentrations of K^+, thus suggesting that its potency and efficacy were much lower than those of Bay K 8644. Finally, Bay K 8644, at variance with MuA, affected $I_{Ba1.2}$ kinetics and stimulated $I_{Ba1.2}$ maximally at weak depolarization values, causing a leftward shift in the maximum of the current–voltage relationship (Wang *et al.*, 1989; McDonald *et al.*, 1994; Saponara *et al.*, 2008; this paper).

When used at high concentrations, MuA acted mostly as a Ca^{2+} channel blocker. Several pieces of evidence concur to this conclusion. First, MuA reversed the contraction induced by high K^+, in agreement with data already published by Wu *et al.* (1998), this relaxant effect becoming more pronounced at higher depolarization levels (i.e. depending on membrane potential; Bean, 1984; Kuriyama *et al.*, 1995). Vasorelaxation induced by Ca^{2+} channel blockers is directly correlated to the extracellular

concentration of K^+, as it is the case with nifedipine, whose potency increases as the membrane voltage (i.e. the concentration of extracellular K^+) increases (McDonald *et al.*, 1994). Second, MuA-induced relaxation was lower when phenylephrine, instead of a high concentration of K^+, was employed to contract the vessel, in line with the observation that $Ca_v1.2$ channels play only a secondary role in this type of contraction (McFadzean and Gibson, 2002), as observed with nifedipine (Gurney, 1994). Third, it inhibited $I_{Ba1.2}$ in single myocytes isolated from both aorta and tail artery. Because this effect was observed independently of the charge carrier used, a Ca^{2+}-dependent inactivation of the channel subsequent to current stimulation can be ruled out.

In the computational study, where a model of the α_{1C} subunit central pore region was reconstructed to perform *in silico* molecular docking analysis, Bay K 8644, nifedipine and MuA showed favourable free-energy binding values. In particular, those related to dihydropyridines are in agreement with already published data (Cosconati *et al.*, 2007; Tikhonov and Zhorov, 2009; Senatore *et al.*, 2011), thus confirming the validity of the model constructed. The two dihydropyridines used in this study showed similar ΔG values and fitted inside the pocket stabilizing the channel conformation by forming H-bonds with key sensing amino acid residues, as previously established by Zhorov (2013). Conversely, MuA lacked the H-bonds formed by the dihydropyridines and showed a less favourable ΔG value. In agreement with these data, the *in silico* alanine scanning mutagenesis showed that the ΔΔG profile shared by nifedipine and Bay K 8644 was not reproduced for MuA, supporting the hypothesis that MuA and the dihydropyridines shared only some amino acid residues when they docked in the pocket of the channel central pore unit. These results corroborate those obtained *in vitro*. On one hand they clearly point to MuA as a novel ligand of $Ca_v1.2$ channels, able to (i) bind as the reference, dihydropyridine ligands to the pore-forming α_{1C} subunit; (ii) prevent Bay K 8644-induced facilitation of extracellular Ca^{2+} influx; and (iii) partly reverse the effects of Bay K 8644 on current kinetics. On the other hand, the less favourable fit of MuA within the pocket might explain why the drug (i) failed to antagonize nifedipine blockade of the current, unlike Bay K 8644; (ii) displayed a low potency and efficacy; (iii) did not affect $I_{Ba1.2}$ stimulated by Bay K 8644, even if tested at concentrations two orders of magnitude higher; and (iv) was not characterized by a voltage-dependence as well as a sigmoidal concentration-dependence.

When the effects of MuA on vascular and cardiac (Son *et al.*, 2014) $Ca_v1.2$ channels are compared, interesting similarities emerge. In both tissues, in fact, MuA induced a concentration-dependent, nifedipine-sensitive stimulation of $I_{Ba1.2}$, without altering the current kinetics. Additionally, current stimulation was bell-shaped, although the highest concentration assessed in cardiomyocytes was only 200 μM, that is, 2.5-fold lower than that tested in vascular myocytes. On the contrary, vascular preparations seemed to be more sensitive to MuA as the pEC_{50} value was one order of magnitude lower than that recorded in cardiomyocytes. Finally, in cardiomyocytes, MuA stimulation of Ca^{2+} sparks and Ca^{2+} transients depends on PKC activation (Kim *et al.*, 2015), while its modulatory activity on rat tail artery $Ca_v1.2$ channel, where PKC plays a stimulatory role (Navedo *et al.*, 2005), was not significantly affected by the PKC inhibitors GF109203X and Gö6976 (Supporting Information Fig. S2). This finding once more suggests that MuA might directly activate the $Ca_v1.2$ channel in vascular myocytes.

In conclusion, the present findings show that the carbazole alkaloid MuA can be included among the molecules of natural origin capable of modulating the voltage-dependent $Ca_v1.2$ channel in vascular as well as in cardiac (Son *et al.*, 2014) myocytes, by docking at the α_{1C} subunit central pore in a different way from that of the dihydropyridines. Vietnamese medicinal plants represent a valuable source for the discovery of novel pharmacological agents that can be useful in the analysis of the basic structure and function of $Ca_v1.2$ channels.

Acknowledgements

This work was supported by the National Foundation for Science and Technology Development of Vietnam (NAFOSTED; grant No. 104.01-2010.25) and by the Ministero degli Affari Esteri (Rome, Italy), as stipulated by Law 212 (26-2-1992), to the project 'Discovery of novel cardiovascular active agents from selected Vietnamese medicinal plants'. Miriam Durante and Paolo Mugnai received a personal PhD scholarship from the University of Siena. We wish to thank Dr. M. Lenoci for the assistance in some preliminary experiments.

Author contributions

F.F. and N.M.C. designed the research study; T.T.H., P.N.K. and N.T.S. prepared the murrayafoline A; M.D., P. M., O.S. and F.F. carried out the experiments; M.D., O.S. and F.F. analysed the data; F.F., S.S., O.S. and G.S. wrote the paper.

Conflict of interest

The authors declare no conflict of interest.

References

Alexander SPH, Benson HE, Faccenda E, Pawson AJ, Sharman JL, Catterall WA, *et al.* (2013). The Concise Guide to PHARMACOLOGY 2013/14: Ion Channels. Br J Pharmacol 170: 1607–1651.

Altschul SF, Madden TL, Schäffer AA, Zhang J, Zhang Z, Miller W, *et al.* (1997). Gapped BLAST and PSI-BLAST: a new generation of protein database search programs. Nucleic Acids Res 25: 3389–3402.

Anand P, Nagarajan D, Mukherjee S, Chandra N (2014). ABS-Scan: in silico alanine scanning mutagenesis for binding site residues in protein-ligand complex. Version 2. F1000Res 3: 214.

Asano M, Nomura Y (1999). Ca^{2+} buffering action of sarcoplasmic reticulum on Bay K 8644-induced Ca^{2+} influx in rat femoral arterial smooth muscle. Eur J Pharmacol 366: 61–71.

Bean BP (1984). Nitrendipine block of cardiac calcium channels: high-affinity binding to the inactivated state. Proc Natl Acad Sci U S A 81: 6388–6392.

Berendsen HJC, Spoel DVD, Drunen RV (2012). GROMACS: a message-passing parallel molecular dynamics implementation. Comput Phys Commun 91: 43–56.

Bhattacharyya P, Chowdhury BK (1985). Glycozolidal, a new carbazole alkaloid from Glycosmis pentaphylla. J Nat Prod 48: 465–466.

Chakraborty S, Chattopadhyay G, Saha C (2013). A tandem reduction–oxidation protocol for the conversion of 1-keto-1,2,3,4-tetrahydrocarbazoles to carbazoles via tosylhydrazones through microwave assistance: efficient synthesis of glycozoline, clausenalene, glycozolicine, and deoxycarbazomycin B and the total synthesis of murrayafoline A. J Heterocycl Chem 50: 91–98.

Cheng RC, Tikhonov DB, Zhorov BS (2009). Structural model for phenylalkylamine binding to the L-type calcium channels. J Biol Chem 284: 28332–28342.

Cheng RCK, Tickhonov DB, Zhorov BS (2010). Structural modeling of calcium binding in the selectivity filter of the L-type calcium channel. Eur Biophys J 39: 839–853.

Choi H, Gwak J, Cho M, Ryu M-J, Lee J-H, Kim SK, *et al.* (2010). Murrayafoline A attenuates the Wnt/β-catenin pathway by promoting the degradation of intracellular β-catenin proteins. Biochem Biophys Res Commun 391: 915–920.

Cosconati S, Marinelli L, Lavecchia A, Novellino E (2007). Characterizing the 1,4-dihydropyridines binding interactions in the L-type Ca^{2+} channel: model construction and docking calculations. J Med Chem 50: 1504–1513.

Cui CB, Yan SY, Cai B, Yao XS (2002). Carbazole alkaloids as new cell cycle inhibitor and apoptosis inducers from *Clausena dunniana* Levl. J Asian Nat Prod Res 4: 233–241.

Cuong NM, Hung TQ, Sung TV, Taylor WC (2004). A new dimeric carbazole alkaloid from *Glycosmis stenocarpa* roots. Chem Pharm Bull 52: 1175–1178.

Cuong NM, Khanh PN, Huyen PT, Duc HV, Huong TT, Ha VT, *et al.* (2014). Vascular L-type Ca^{2+} channel blocking activity of sulphur-containing indole alkaloids from Glycosmis petelotii. J Nat Prod 77: 1586–1593.

Furukawa H, Wu TS, Ohta T, Kuoh CS (1985). Chemical constituents of Murraya euchrestifolia HAYATA. Structures of novel carbazolequinones and other new carbazole alkaloids. Chem Pharm Bull 33: 4132–4138.

Fusi F, Saponara S, Frosini M, Gorelli B, Sgaragli G (2003). L-type Ca^{2+} channels activation and contraction elicited by myricetin on vascular smooth muscles. Naunyn Schmiedebergs Arch Pharmacol 368: 470–478.

Fusi F, Saponara S, Gagov H, Sgaragli GP (2001). 2,5-Di-*t*-butyl-1,4-benzohydroquinone (BHQ) inhibits vascular L-type Ca^{2+} channel via superoxide anion generation. Br J Pharmacol 133: 988–996.

Fusi F, Sgaragli G, Ha LM, Cuong NM, Saponara S (2012). Mechanism of osthole inhibition of vascular $Ca_v1.2$ current. Eur J Pharmacol 680: 22–27.

Guex N, Peitsch MC (1997). SWISS-MODEL and the Swiss-PdbViewer: an environment for comparative protein modeling. Electrophoresis 18: 2714–2723.

Gurney AM (1994). Mechanisms of drug-induced vasodilation. J Pharm Pharmacol 46: 242–251.

Hamill OP, Marty A, Neher E, Sakmann B, Sigworth FJ (1981). Improved patch-clamp techniques for high-resolution current recording from cells and cell-free membrane patches. Pflugers Arch 391: 85–100.

Hess P, Lansman JB, Tsien RW (1984). Different modes of Ca channel gating behaviour favoured by dihydropyridine Ca agonists and antagonists. Nature 311: 538–544.

Ito C, Itoigawa M, Nakao K, Murata T, Kaneda N, Furukawa H (2012). Apoptosis of HL-60 leukemia cells induced by carbazole alkaloids isolated from *Murraya euchrestifolia*. J Nat Med 66: 357–361.

Itoigawa M, Kashiwada Y, Ito C, Furukawa H, Tachibana Y, Bastow KF, *et al.* (2000). Antitumor agents. 203. Carbazole alkaloid murrayaquinone A and related synthetic carbazolequinones as cytotoxic agents. J Nat Prod 63: 893–897.

Jiang Y, Lee A, Chen J, Ruta V, Cadene M, Chait BT, *et al.* (2003). X-ray structure of a voltage-dependent K^+ channel. Nature 423: 33–41.

Kilkenny C, Browne W, Cuthill IC, Emerson M, Altman DG (2010). Animal research: reporting *in vivo* experiments: the ARRIVE guidelines. Br J Pharmacol 160: 1577–1579.

Kim JC, Wang J, Son MJ, Cuong NM, Woo SH (2015). Sensitization of cardiac Ca^{2+} release sites by protein kinase C signaling: evidence from action of murrayafoline A. Pflügers Arch 467: 1607–1621.

Kuriyama H, Kitamura K, Nabata H (1995). Pharmacological and physiological significance of ion channels and factors that modulate them in vascular tissues. Pharmacol Rev 47: 387–573.

Laskowski RA, MacArthur MW, Moss DS, Thornton JM (1993). PROCHECK – a program to check the stereochemical quality of protein structures. J Appl Cryst 26: 283–291.

McDonald TF, Pelzer S, Trautwein W, Pelzer DJ (1994). Regulation and modulation of calcium channels in cardiac, skeletal, and smooth muscle cells. Physiol Rev 74: 365–507.

McFadzean I, Gibson A (2002). The developing relationship between receptor-operated and store-operated calcium channels in smooth muscle. Br J Pharmacol 135: 1–13.

McGrath J, Drummond G, McLachlan E, Kilkenny C, Wainwright C (2010). Guidelines for reporting experiments involving animals: the ARRIVE guidelines. Br J Pharmacol 160: 1573–1576.

Morris GM, Huey R, Lindstrom W, Sanner MF, Belew RK, Goodsell DS, *et al.* (2009). AutoDock and AutoDockTools: automated docking with selective receptor flexibility. J Comput Chem 30: 2785–2791.

Mugnai P, Durante M, Sgaragli G, Saponara S, Paliuri G, Bova S, *et al.* (2014). L-type Ca^{2+} channel current characteristics are preserved in rat tail artery myocytes after one-day storage. Acta Physiol 211: 334–345.

Navedo MF, Amberg GC, Votaw VS, Santana LF (2005). Constitutively active L-type Ca^{2+} channels. Proc Natl Acad Sci U S A 102: 11112–11117.

NCBI Protein Database. Available at: http://www.ncbi.nlm.nih.gov/protein/ (http://www.ncbi.nlm.nih.gov/protein/) (accessed 7/20/2015).

Pawson AJ, Sharman JL, Benson HE, Faccenda E, Alexander SP, Buneman OP, *et al.* (2014) The IUPHAR/BPS Guide to PHARMACOLOGY: an expert-driven knowledge base of drug targets and their ligands. Nucl. Acids Res. 42 (Database Issue): D1098–1106.

PubChem database. Available at: http://www.ncbi.nlm.nih.gov/pcsubstance/ (http://www.ncbi.nlm.nih.gov/pcsubstance/) (accessed 7/20/2015).

Saponara S, Sgaragli G, Fusi F (2008). Quercetin antagonism of Bay K 8644 effects on rat tail artery L-type Ca^{2+} channels. Eur J Pharmacol 598: 75–80.

Senatore A, Boone A, Lam S, Dawson TF, Zhorov B, Spafford JD (2011). Mapping of dihydropyridine binding residues in a less sensitive invertebrate L-type calcium channel (LCa_v1). Channels 5: 173–187.

Son M-J, Chidipi B, Kim J-C, Huong TT, Tai BH, Kim YH, *et al*. (2014). Alterations of contractions and L-type Ca^{2+} currents by murrayafoline-A in rat ventricular myocytes. Eur J Pharmacol 740: 81–87.

Sorin EJ, Pande VS (2005). Exploring the helix-coil transition via all-atom equilibrium ensemble simulations. Biophys J 88: 2472–2493.

Stansfeld C, Mathie A (1993). Recording membrane currents of peripheral neurones in short-term culture. In: (ed)Wallis DI. Electrophysiology A Practical Approach. IRL Press: Oxford, pp. 3–28.

Thuy TT, Cuong NM, Toan TQ, Thang NN, Tai BH, Nhiem NX, *et al*. (2013). Synthesis of novel derivatives of murrayafoline A and their inhibitory effect on LPS-stimulated production of pro-inflammatory cytokines in bone marrow-derived dendritic cells. Arch Pharm Res 36: 832–839.

Tikhonov DB, Zhorov BS (2009). Structural model for dihydropyridine binding to L-type calcium channels. J Biol Chem 284: 19006–19017.

Toan TQ, Thuy TTT, Khanh PN, Ha ĐT, Cuong NM (2013). Research on total synthesis of murrayafoline A. Vietnam J Chem 51: 91–94.

Trott O, Olson AJ (2010). AutoDock Vina: improving the speed and accuracy of docking with a new scoring function, efficient optimization, and multithreding. J Comput Chem 31: 455–461.

Usowicz MM, Gigg M, Jones LM, Cheung CW, Hartley SA (1995). Allosteric interactions at L-type calcium channels between FPL 64176 and the enantiomers of the dihydropyridine Bay K 8644. J Pharmacol Exp Ther 275: 638–645.

Wang R, Karpinski E, Pang PK (1989). Two types of calcium channels in isolated smooth muscle cells from rat tail artery. Am J Physiol 256: H1361–H1368.

Wu T-S, Chan Y-Y, Liou M-J, Lin F-W, Shi L-S, Chen K-T (1998). Platelet aggregation inhibitor from *Murraya euchrestifolia*. Phytother Res 12 (Suppl. 1): S80–S82.

Zhao W, Zhang J, Lu Y, Wang R (2001). The vasorelaxant effect of H(2)S as a novel endogenous gaseous K(ATP) channel opener. EMBO J 20: 6008–6016.

Zhorov BS (2013). Interactions of drugs and toxins with permanent ions in potassium, sodium, and calcium channels. Neurosci Behav Physiol 43: 388–400.

Zhorov BS, Tikhonov DB (2004). Potassium, sodium, calcium and glutamate-gated channels: pore architecture and ligand action. J Neurochem 88: 782–799.

Supporting Information

Additional Supporting Information may be found in the online version of this article at the publisher's web-site:

http://dx.doi.org/10.1111/bph.13369

Figure S1 Effect of murrayafoline A on phenylephrine-induced contraction of rat aorta rings. Concentration-response curves of MuA in endothelium-denuded rings precontracted by 0.3 M phenylephrine. In the ordinate scale, response is reported as percentage of the initial tension induced by phenylephrine (phe), taken as 100%. Data points are mean ± SEM (n = 6).

Figure S2 Murrayafoline A modulation of Ba1.2 of single rat tail artery myocytes. Effect of GF109203X and Gö6976 on MuA-induced modulation of Ba1.2. Concentration-dependent effect of MuA measured at Vh of −50 mV in the absence (control) or presence of either 5 μM GF109203X or 100 nM Gö6976. On the ordinate scale, response is given as a percentage of control. Data points are mean ± SEM. (n = 5–9). * $P < 0.05$ vs. control (100%), one sample *t* test.